Effect of anodization and loading on fatigue life of 2618-T851 aluminum alloy

Benaïssa Malek, Michel Chaussumier, Catherine Mabru

Effect of anodization and loading on fatigue life of 2618-T851 aluminum alloy

Benaïssa Malek · Michel Chaussumier · Catherine Mabru

Abstract Anodizing process is largely performed on aluminum alloys to enhance corrosion and wear resistances. However, this process can significantly reduce the fatigue resistance of aluminum alloys depending on the alloy and the process parameters. This paper deals with the influence of anodizing process on fatigue resistance of the aeronautical aluminum alloy 2618-T851. The anodic film has been characterized after each step using scanning electron microscopy (SEM). This analysis showed that the anodic layer was crazed just after impregnation operation with micro-cracks extending from the surface up to half the anodic layer. Simultaneously, uniaxial fatigue tests under tension or torsion loadings have been conducted in order to evaluate the effect of each process step in relation with loading nature. The results showed that the anodizing step has a detrimental effect on fatigue life of 2618 alloy when specimens are subjected to tensile loading. However, anodizing process has no effect on fatigue life under torsion loading. Fractographic observations have been conducted in order to get an insight on the mechanisms involved in each case.

B. Malek (✉) · M. Chaussumier · C. Mabru
Université de Toulouse, Institut Clément Ader (ICA), UMR CNRS 5312, UPS/INSA/ISAE/Mines Albi, 3 rue Caroline Aigle, 31400 Toulouse, France
e-mail: bnssmalek@gmail.com

Keywords 2618-T851 · Anodizing · Fatigue · Tension · Torsion

1 Introduction

Aluminum alloys are widely used in aircraft construction. When they are exposed to an aggressive environment, the natural oxide film that forms on the surface is not sufficient to protect the structure from corrosion. Anodic oxidation is then used to improve wear and corrosion resistances (Mehdizade et al. 2019; Darmawan et al. 2018; Lu et al. 2018). In addition, sealing operation could be done after anodizing to improve corrosion resistance (Wang et al. 2019; Canyook et al. 2018; Zhang et al. 2018; Mason et al. 2011). However, fatigue life of such treated specimens is often reduced (Kudari and Sharanaprabhu 2018; Zhao et al. 2015; Crawford 2013; Nie et al. 2013; Shahzad et al. 2010a, b, 2011a, b; Lonyuk et al. 2007). Indeed, anodizing process affects the surface characteristics of the parts; composition, roughness, as well as internal stresses can be modified. All these surface parameters are known to be involved in the fatigue resistance (Boyer et al. 2007; James et al. 2007). Moreover, the brittle nature of the anodic film can also interfere in the mechanisms leading to the decrease of fatigue resistance. Many research studies have been conducted on this topic. For instance, the effects of

chromic and sulfuric anodizing on the very high cycle fatigue behavior during purely reversed fatigue tests of 2A12 have been investigated (Nie et al. 2013). It has been shown that the decrease of the fatigue life is related to cracks initiating from the interface between the anodic film and the substrate whatever the acid used. In the case of sulfuric anodizing, the effect is attributed to the cracking of the anodic layer and the overgrowth of the oxide film into the substrate. For the case of chromic anodizing, early cracking is due to tensile residual stress in the interface. The decrease in tensile fatigue life for anodized-sealed specimens of 2214-T6 anodized in sulfuric acid as compared to bare condition is due to a decrease in initiation period and multi-site crack initiations as a result of the formation of cavities due to the dissolution of coarse Al_2Cu particles during anodization and network of micro-cracks on anodic film surface initiated during sealing process (Shahzad et al. 2011a, b). Anodizing process parameters (such as time, temperature and voltage) can affect the fatigue resistance. This has been investigated for 2024-T3 alloy anodized in a mixed solution of sulfuric and tartaric acids under tensile fatigue tests; increasing the voltage leads to a decrease of the fatigue life, suggesting the thickness of the anodic layer must be taken into account (Zhao et al. 2015). This has been confirmed by a study on 7075-T6 alloy anodized in sulfuric acid for various periods of time, leading to various oxide layer thicknesses. The negative effect of anodizing on rotating-bending fatigue life is more important for the thickest coating layer (Cirik and Genel 2008). Varying time, temperature and voltage during chromic acid anodizing of 2024-T351 modifies the reversed tensile fatigue life reduction as compared to untreated specimens (Kudari and Sharanaprabhu 2018). Sometimes, anodizing step is not the only key step of the process that causes fatigue life decrease. A detrimental effect of the pickling step, prior to the anodizing one, has been noted on the fatigue resistance of 2024-T351 (Kudari and Sharanaprabhu 2018), 7010 (Shahzad et al. 2010a, b) and 7050 (Shahzad et al. 2011a, b). For these last two alloys, it has been shown that pickling results in pits formation at the surface, accelerating fatigue crack nucleation and promoting multi-site crack initiation. The pickling step completely changed the crack initiation mechanisms as compared to non-treated specimens, leading to a drastic degradation of the fatigue life. The small decrease in fatigue life of anodized specimens as compare to pickled specimens was attributed to brittle nature and micro-cracking of the coating.

At last, for a given alloy and a given surface treatment, the effects of the anodizing process can depend on the microstructural state of the alloy, as for 2017 A (Fares et al. 2015). In addition, the nature of the loading seems to have an influence on the effect of anodizing process on fatigue resistance (Shiozawa et al. 2000); fatigue resistance of anodized specimen of 2014-T6 tested in tension decreased as compared with that of bare specimens. But no effect on fatigue resistance has been shown under purely reversed rotating-bending fatigue test.

In this context, the aim of the present paper is to characterize the effect of a given anodizing process on the fatigue resistance of 2618-T851 aluminum alloy largely used in the past, especially in well-known Concorde aircraft. The alloy knows a slight decrease of fatigue resistance at high temperature compared to room temperature fatigue resistance (Doyle 1969; Williams and Starke 2003). A careful analysis of the surface has been conducted after each step and correlated to fracture surface observations and special attention is paid to the potential influence on the fatigue life of each step of the whole process under uniaxial loading.

2 Experimental details

The material investigated in this study is 2618-T851 aluminum alloy. The chemical composition is given in Table 1. It can be seen, among addition elements, there is a high content of iron and nickel. The mechanical properties in pure tension and pure torsion have been determined using a MTS multiaxial fatigue machine. The results are given in Table 2. Tensile results were found to be in good agreement with values found in literature (Wang et al. 2008; Khalil and Lang 2011; Bathias et al. 1981; Aghaie-Khafri and Zargaran 2010).

Specimens have been machined in a laminated plate of 2618-T851 aluminum alloy. After the laminating process, the plate has been heated at a solution treatment temperature (530 ± 5 °C), water quenched and tempered at 190 °C during 20 h. It is then hot worked by tension and finally quenched and tempered at 200 °C during some minutes.

Table 1 Chemical composition (at%) of 2618-T851 aluminum alloy

Cu	Zn	Mg	Fe	Si	Mn	Ti	Ni	Al
0.9–1.5	< 0.1	1.35–2	0.4–0.6	0.2	< 0.15	0.15	0.2–0.6	Balance

Table 2 Mechanical properties of 2618-T851 aluminum alloy

Young's modulus, E (GPa)	Ultimate tensile stress (MPa)	Tensile yield stress at 0.2% (MPa)	Compressive yield stress (MPa)	Shear modulus, G (GPa)	Shear yield stress at 0.2% (MPa)	Ratio σ_y/τ_y
72	464	438	400	27	260	1.69

The microscopic observation of the microstructure has shown the presence of coarse intermetallic particles in grains and grain boundaries, aligned along the laminate direction (Fig. 1); the mean size of these particles is of 15 μm in longitudinal direction, 12 μm in the two other directions. It has been found that the coarse intermetallic particles correspond to Al_9FeNi. Finest Al_2Cu hardening particles have been also detected. These observations are in good agreement with microstructural observations made by other researchers (Özbek 2007; Novy et al. 2009).

Uniaxial tensile and torsion fatigue tests were performed at room temperature using cylindrical specimens (Fig. 2) with an arithmetic roughness of 0.8 μm, under a frequency of 10 Hz, with a stress ratio of 0.1 for tensile tests and − 1 for torsion tests.

The fatigue loading levels have been chosen to study the fatigue behavior of 2618 alloy in the cycle fatigue domain between 10^4 cycles and 10^7 cycles. The nominal stresses used in tensile and torsion fatigue tests are respectively in the range of 80 MPa to 200 MPa and 70 MPa to 200 MPa.

Prior to anodizing, degreasing and pickling are two necessary pretreatments; the objective is to produce a chemically clean surface ready to be anodized. Impregnation and sealing were used after anodizing in order to obtain good wear and corrosion resistances. The whole process is described in Table 3.

3 Results and discussion

3.1 Surface characterization

As noted in the introduction, the pickling step of the anodizing process has sometimes been identified as the main step causing the decrease of the fatigue resistance of an anodized aluminum alloy (Shahzad et al. 2010a, b, 2011a, b). This was attributed to the presence of pits on the surface resulting from the pickling. These pits acts as stress concentrators and promote crack initiation. In the case of 2618-T851 aluminum alloy, Fig. 3 obtained by scanning electron microscopy (SEM) shows that Al_9FeNi particles still remain at the surface but the substrate around has been preferentially attacked creating cavities around these particles. The surface size of these cavities can reach 10 μm. However, the average roughness is only slightly affected as roughness measurements give an arithmetic roughness of 0.9 μm compared to 0.8 μm in the as-machined conditions.

Anodizing step is an electrochemical treatment that improves wear and corrosion resistances by developing a controlled anodic film in the surface. A cross section and the surface view of the anodic film are shown in Fig. 4. The thickness of the anodic layer is about 9 μm. The surface is not homogenous. A high density of cavities can be observed at the surface and within the oxide layer (Fig. 5). This is due to the presence of various and numerous coarse intermetallic phases in the aluminum matrix. Depending on their electrochemical behavior towards the aluminum matrix, these micro-sized particles can induce the formation of holes because they dissolve under anodizing conditions or can be incorporated in the anodic layer, inducing a modification of the alumina density above the particle (Veys-Renaux et al. 2016).

Despite the numerous surface defects, the average arithmetic roughness is unchanged compared to the previous step and is still of 0.9 μm. The impregnation step follows the anodization step and was achieved by immersing the parts in a chemical solution based on

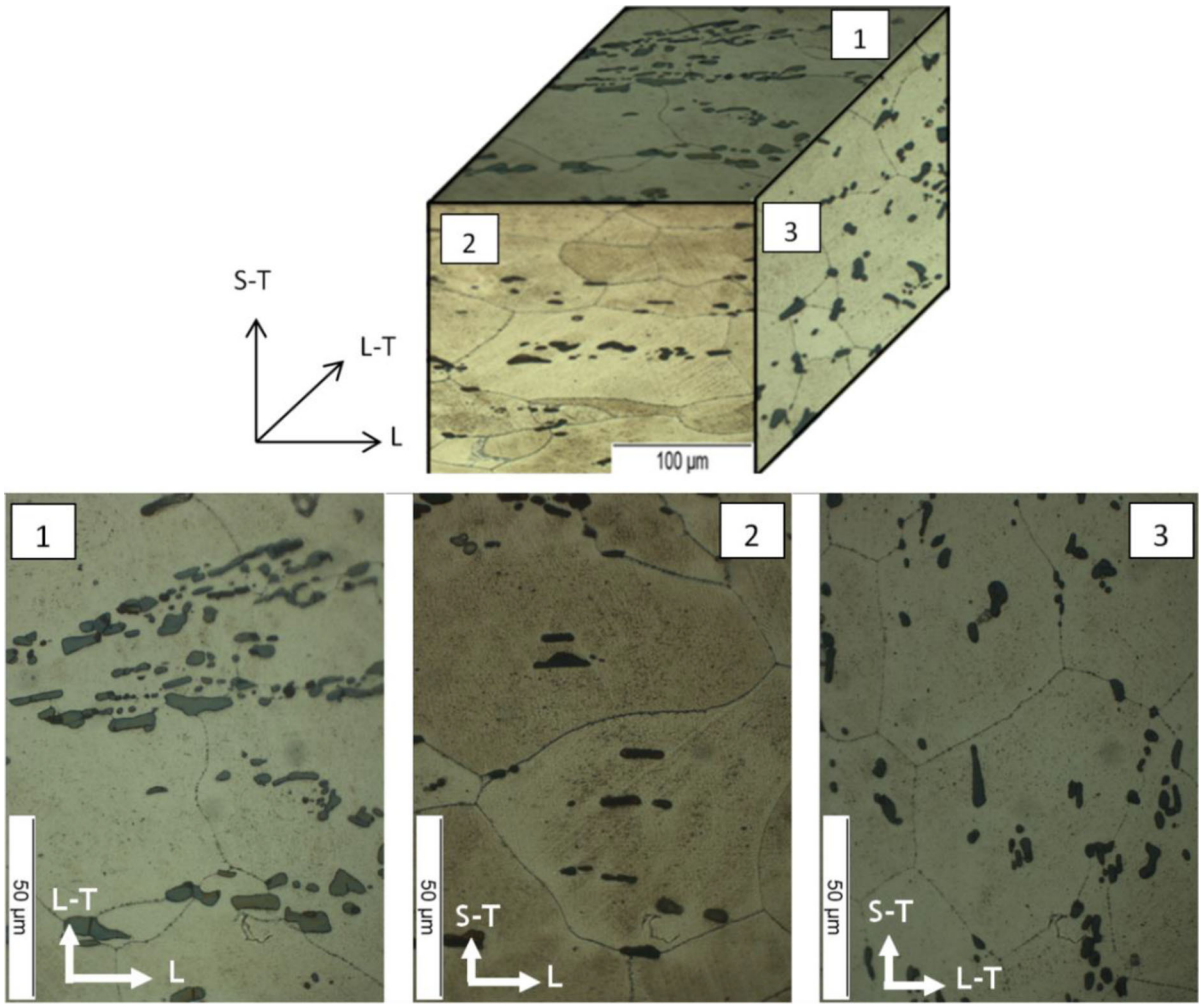

Fig. 1 3D microstructure of 2618-T851 aluminum alloy (*L* laminated direction, *L-T* long-transverse direction, *S-T* short-transverse direction)

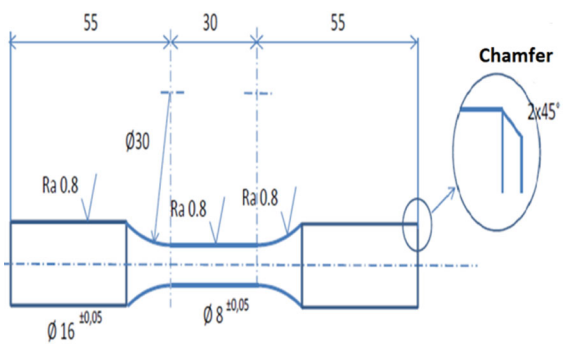

Fig. 2 Geometry of specimens for fatigue test (dimensions are in mm)

trivalent chromium and zirconium. Surface and cross-section views of the anodic film after impregnation are presented in Fig. 6. After impregnation the surface still presents a high density of defects. The density of surface defects is similar to what was observed before impregnation and the arithmetic roughness is still of 0.9 µm. In addition, the anodic film is crazed. The depth of the micro-cracks within the anodic film is almost half of the layer thickness. This might be related to the presence of Zirconium and Chromium observed in the upper part of the anodic layer (see Fig. 7). The atomic content of zirconium and chromium was determined by a linear EDX analysis of the chemical composition of the anodic layer from the

Table 3 Parameters of the surface treatment process of 2618-T851 alloy

Process	Bath nature	Temperature (°C)	Time (min)
Degreasing	Sococlean A3431 10%	45	6
Pickling	Socosurf A1858/A1806	50	10
Anodization	Sulfuric acid 200 g/L (15 V)	18	40
Impregnation	Lanthane 613.3	40	20
Sealing	H_2O	98–100	30

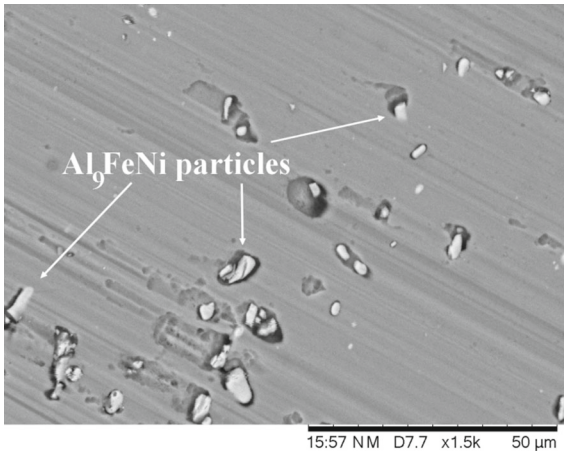

Fig. 3 Surface of 2618 specimens after pickling

aluminum/coating interface layer to the outer surface of the anodic layer as indicated in Fig. 5 by the arrow.

Figure 7 shows the presence of zirconium and chromium which is consistent with the composition of the impregnation solution. The atomic content of the zirconium and chromium reach respectively 1% and 0.7% in the middle of the anodic layer which corresponds to the beginning of the anodic film crazing. In the outer layer, the content is respectively 12% and 3%.

It has been reported in some studies that such micro-cracks can be explained by the thermal expansion coefficient mismatch between the anodic layer and the aluminum substrate (Liu et al. 2008; Goueffon et al. 2009; Côté et al. 2014).

The volume of the compounds formed during this impregnation step can also create stresses that cause cracks. This gradient of composition can also be the cause of a gradient of mechanical properties (toughness, ultimate strength…). The same micro-cracks appear in some metallic materials (Liu et al. 2008; Schuster et al. 2015). Additional mechanical–physical–chemical characterizations should be performed to formally establish the reasons for this type of crazing.

Micro-cracks delineate irregular cells more or less closed in polygonal shape. The average size of the cells is 20 µm, their surface area and density are

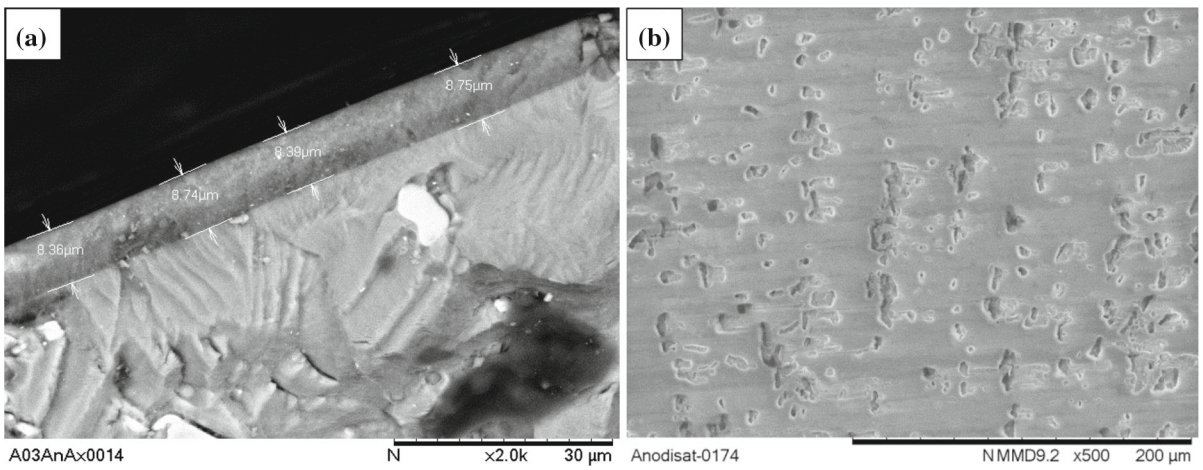

Fig. 4 **a** Cross section and **b** surface view of anodic film of anodized specimen

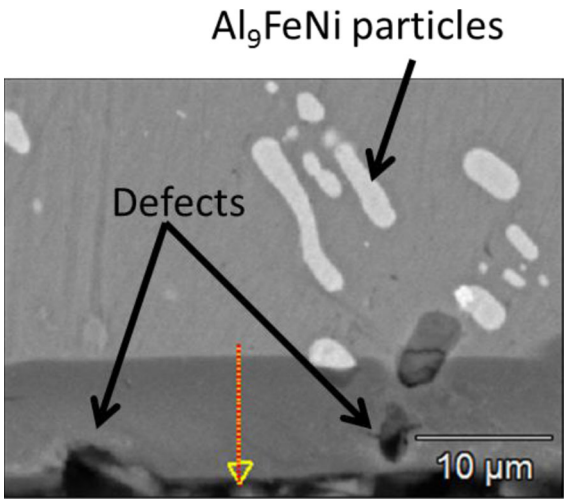

Fig. 5 Defects in the anodic film

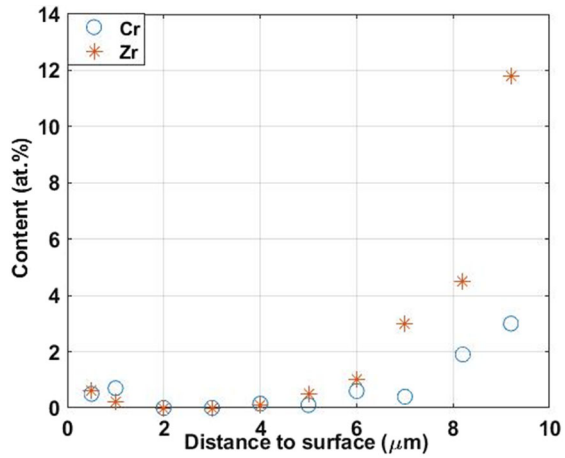

Fig. 7 Zirconium and Chromium content through the thickness of the anodic film by EDX analysis

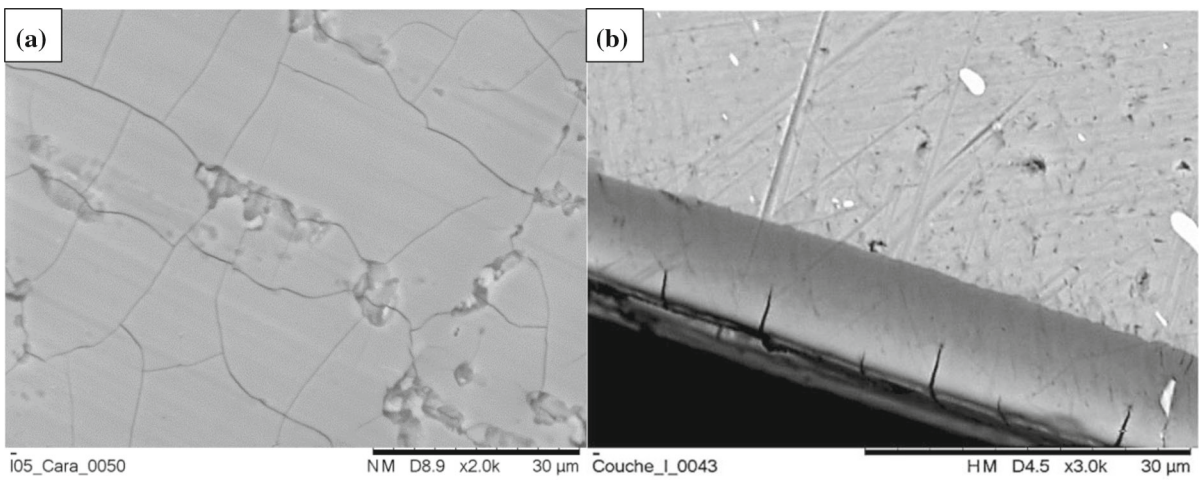

Fig. 6 **a** Surface and **b** cross-section views of anodic film after impregnation

respectively equal to 350 μm^2 and 3×10^{-3} per μm^2 on a representative area of 100 × 100 µm × µm.

The last step is sealing in boiling water. Surface and cross-section views of the anodic film after sealing are shown in Fig. 8. Surface defects and crazing similar to the previous step can be observed. However, cross-section observations show that some micro-cracks that appeared during impregnation step propagated throughout the anodic layer and reach the substrate. In addition, the cells created by these micro-cracks are smaller (surface area of about 150 μm^2), with a higher density 7.5×10^{-3} per μm^2 indicating that this sealing step results not only in propagating existing cracks through the thickness layer but also in the creation of new cracks.

In a previous study, the triptych microstructure, microgeometry and residual stresses influencing fatigue resistance was investigated and it has been shown that the fatigue life of 2618 aluminum alloy is only sensitive to its microstructure. The main purpose of residual stress measurement, in this paper, is to study their evolution after each step of the anodizing treatment. Residual stresses of the specimen surfaces have been determined thanks to DRX measurements. The results for the initial surface (machined) and after each step of the surface treatment are presented in

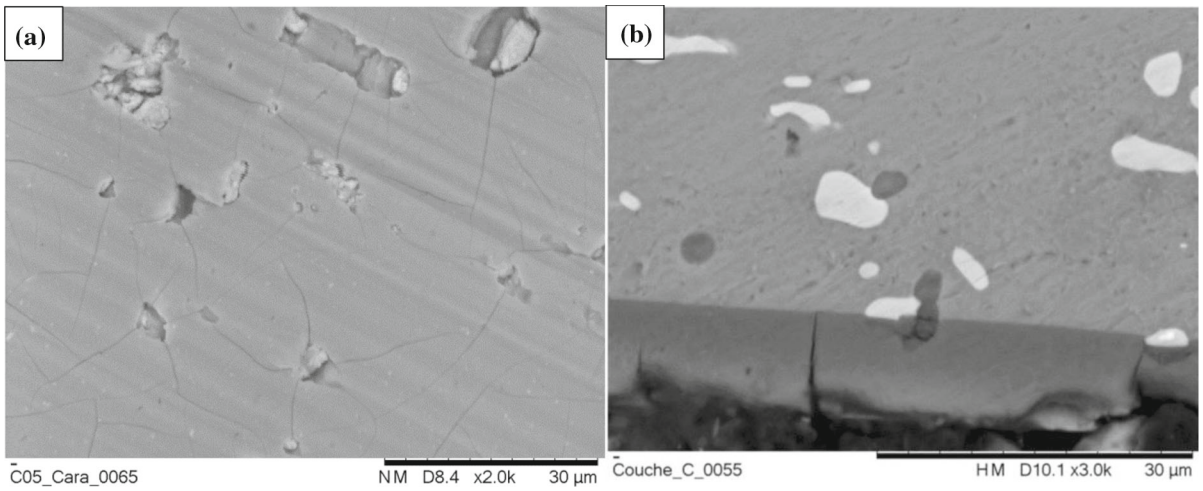

Fig. 8 **a** Surface and **b** cross-section views of anodic film after sealing

Fig. 9. The values are quite low and taking into account the uncertainty (about ± 70 MPa), no difference between the various steps can be highlighted. As a consequence, among the parameters that can control the fatigue resistance and that can be affected by the surface treatment process, residual stresses will be neglected compared to microstructure and microgeometry of the surface.

3.2 Tensile fatigue tests

Tensile fatigue tests have been performed on surface treated and as machined specimens under a stress ratio of R_s ($R_s = \frac{\sigma^{min}}{\sigma^{max}} = 0.1$). The stress ratio of 0.1 has been chosen because it is a conventional stress ratio used in aeronautical fatigue investigations and also to extend experimental investigation range and include a mean normal stress.

Figure 10 shows the obtained results.

Contrary to what could be expected (creation of surface cavities that could affect the fatigue life James 2007; Cirik and Genel 2008), pickling does not reduce the fatigue life. A degrading effect of anodizing step can be observed. No additional fatigue life reduction is observed for impregnated and sealed specimens.

Fracture surface analysis have been conducted in order to identify the mechanisms involved in the failure for each step of the surface treatment. For machined and pickled specimens, the fatigue cracks initiated from a single site at the surface. The crack initiation is attributed to the coarse intermetallic particles that act as stress concentrators (Figs. 11, 12). For anodized, impregnated and sealed specimens the

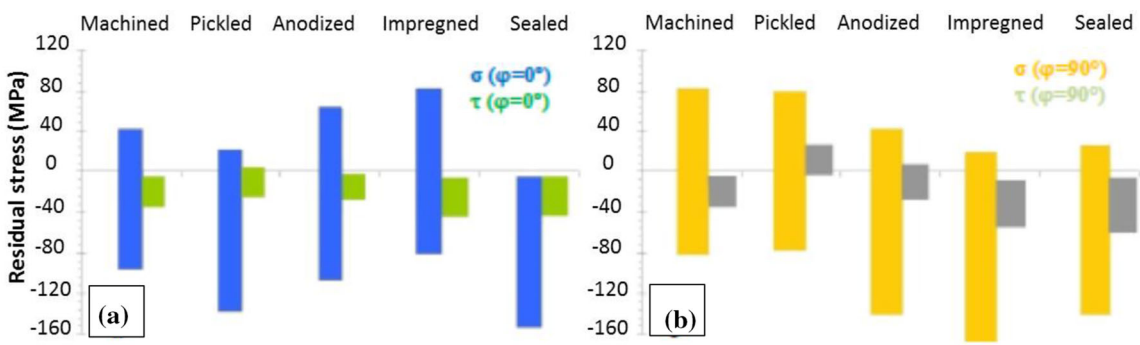

Fig. 9 Maximal surface residual stresses determined after each step of the surface treatment. **a** φ = 0° and **b** φ = 90°

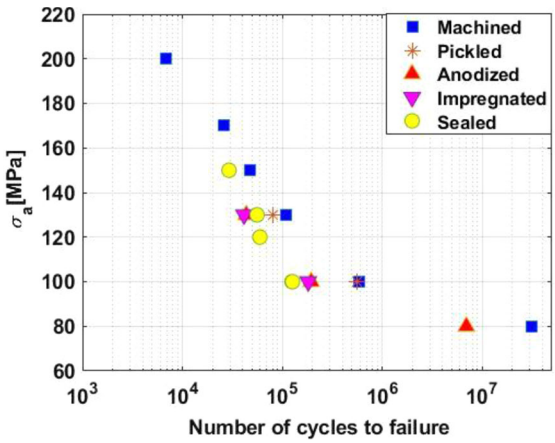

Fig. 10 Effect of surface treatment on tensile fatigue life

anodic film is identified to be involved in the fatigue failure of treated specimens. The fatigue cracks initiated from multi-sites situated on the surface. SEM observations of fracture surfaces of anodized, impregnated and sealed specimens are presented in Figs. 13, 14 and 15 respectively.

No particles are found on the initiation sites. However, numerous cracks of the anodic layer, penetrating into the substrate, can be systematically found, even for the anodized specimen whose oxide layer was not cracked prior to test. The presence of coarse intermetallic particles and associated defects in the anodic film can be observed sometimes and could also contribute to crack initiation. As the fatigue lives of anodized, impregnated and sealed specimens are similar, the micro-cracks that appeared during the process of impregnation and develop during the process of sealing before fatigue test seem to have a negligible effect.

3.3 Torsion fatigue tests

The same approach was followed to determine the effect of each step of the anodizing process on the fatigue resistance of 2618-T851 under torsional loading. Torsional fatigue tests have been performed on treated and untreated specimens in purely reversed torsion. The obtained results are presented in Fig. 16.

As shown, no influence of the surface treatment on fatigue resistance of 2618-T851 is observed, whatever the step of the process. Surface fracture analyses of specimens tested in torsion is sometimes difficult. Indeed, during the last cycles before the final failure, fracture surfaces rub in certain areas generating deformation due to friction (Fig. 17), which sometimes complicates the observation of the crack initiation sites.

However, it was possible to observe some of these specimens tested in torsion. Figure 18 shows the initiation site of a machined specimen.

It appears that fatigue cracks initiated from a single site at the surface crack initiation zone contain coarse intermetallic particles that act as stress concentrators. Mechanisms seem similar to those observed for as machined specimens tested in tension.

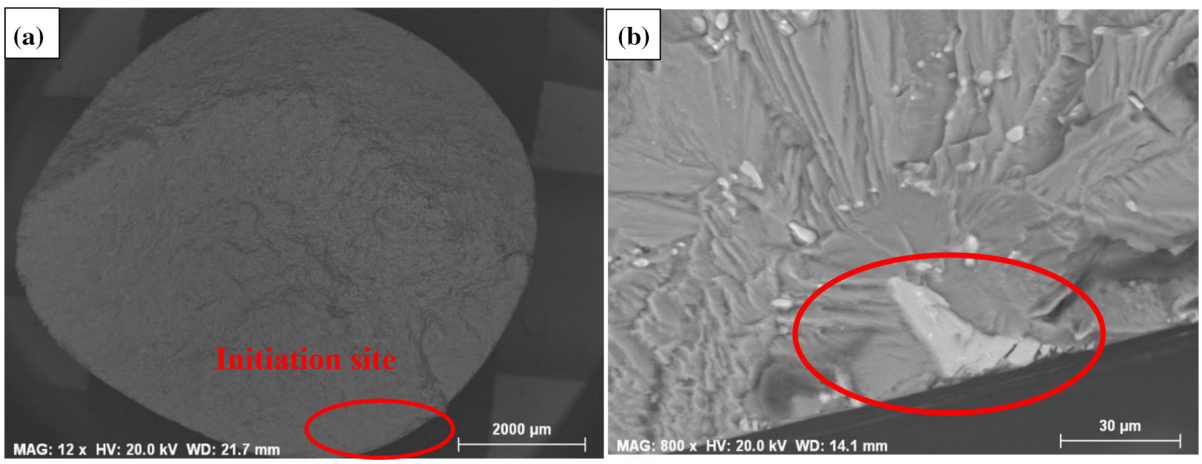

Fig. 11 Initiation sites of machined specimen, σ_a = 130 MPa. **a** Full view of fracture and **b** initiation site localization

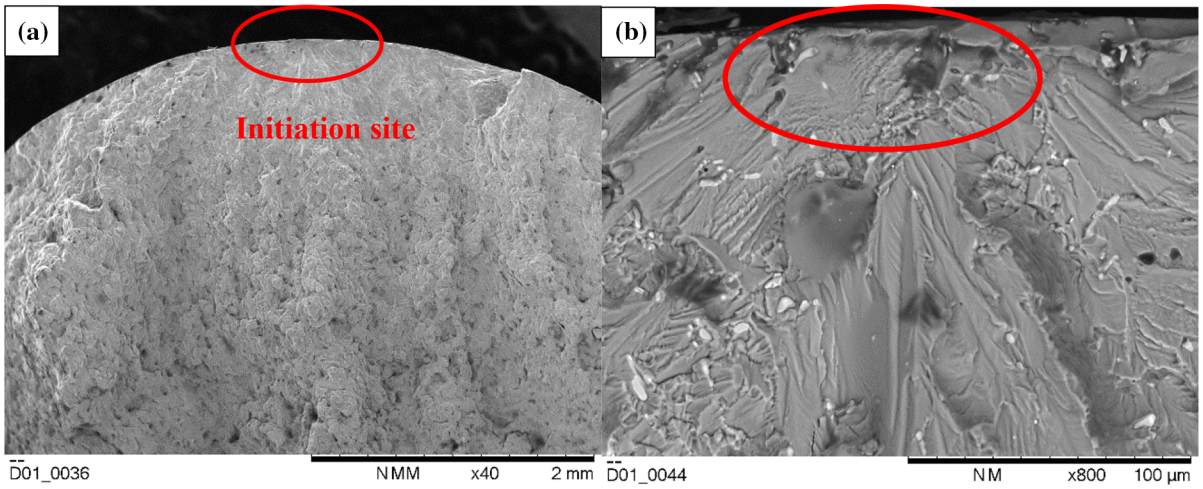

Fig. 12 Initiation sites of pickled specimen, σ_a = 130 MPa. **a** Semi view of fracture and **b** initiation site localization

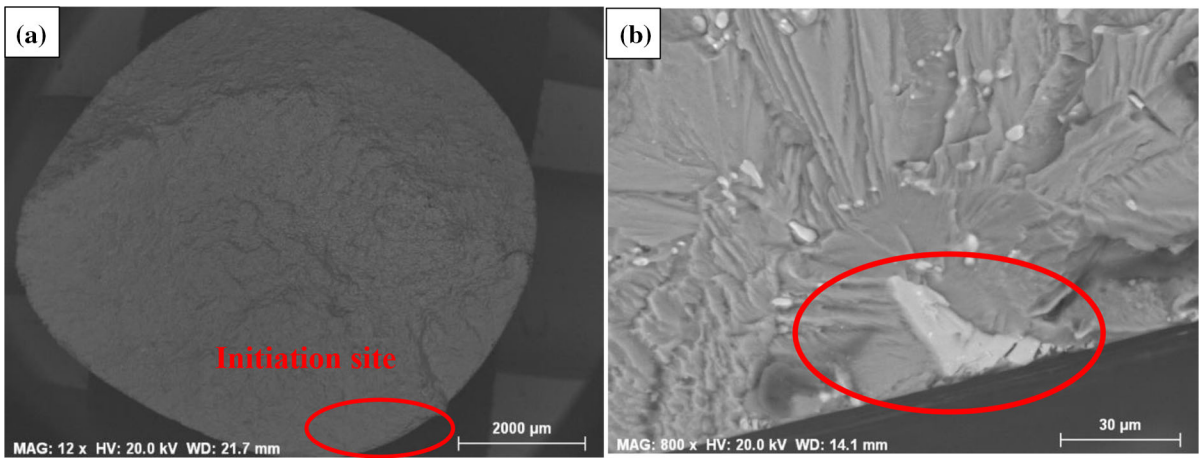

Fig. 13 Initiation sites of anodized specimen, σ_a = 130 MPa. **a** Full view of fracture and **b** initiation site localizations

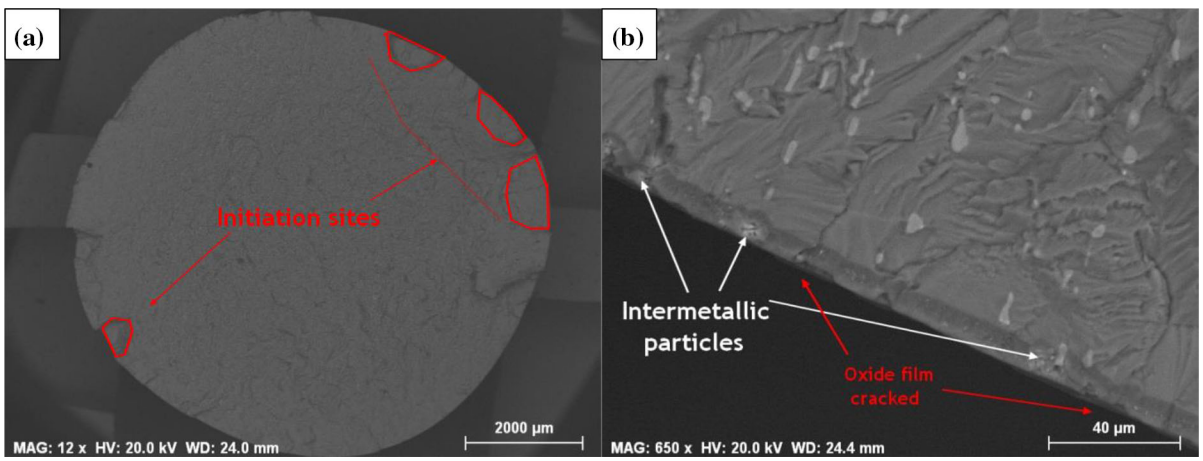

Fig. 14 Initiation sites of impregnated specimen, σ_a = 130 MPa. **a** Full view of fracture and **b** initiation site localizations

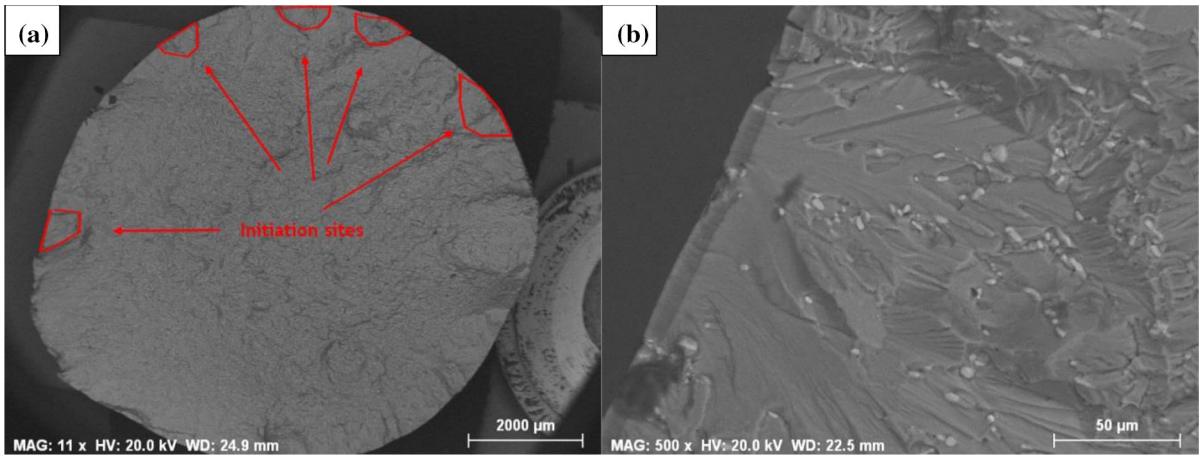

Fig. 15 Initiation sites of sealed specimen, σ_a = 130 MPa. **a** Full view of fracture and **b** initiation site localizations

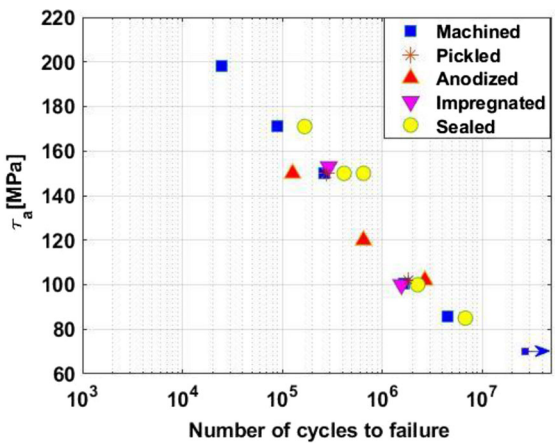

Fig. 16 Effect of surface treatment on torsion fatigue life

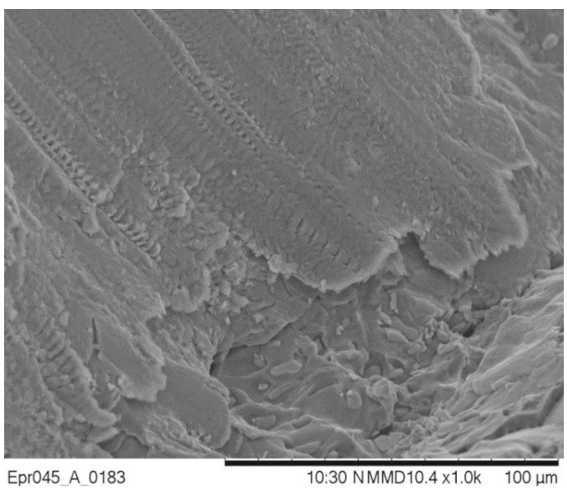

Fig. 17 Deformed area of a fracture surface, as machined specimen, τ_a = 85 MPa

Unfortunately for the treated specimens, it was not possible to conclude on the mechanisms involved in crack initiation due to the rubbing of the fracture surfaces.

4 Conclusion

(1) For machined and pickled specimens, the crack initiation from a single site is attributed to the coarse intermetallic particles Al_9FeNi acting as stress concentrators.
(2) For treated specimens, a reduction of fatigue life for tensile loading is observed.
(3) Anodizing is the detrimental step of the whole surface treatment process leading to a fatigue life reduction in tensile loading; this time, the cracking of the oxide film is identified as the origin of multi-sites.
(4) The impregnation and sealing steps do not generate additional reduction of fatigue life, despite the crazing observed early in which some micro-cracks overgrow the substrate.
(5) Anodizing process does not affect fatigue life under torsional loading; the cracks systematically begin on the surface from Al_9FeNi.

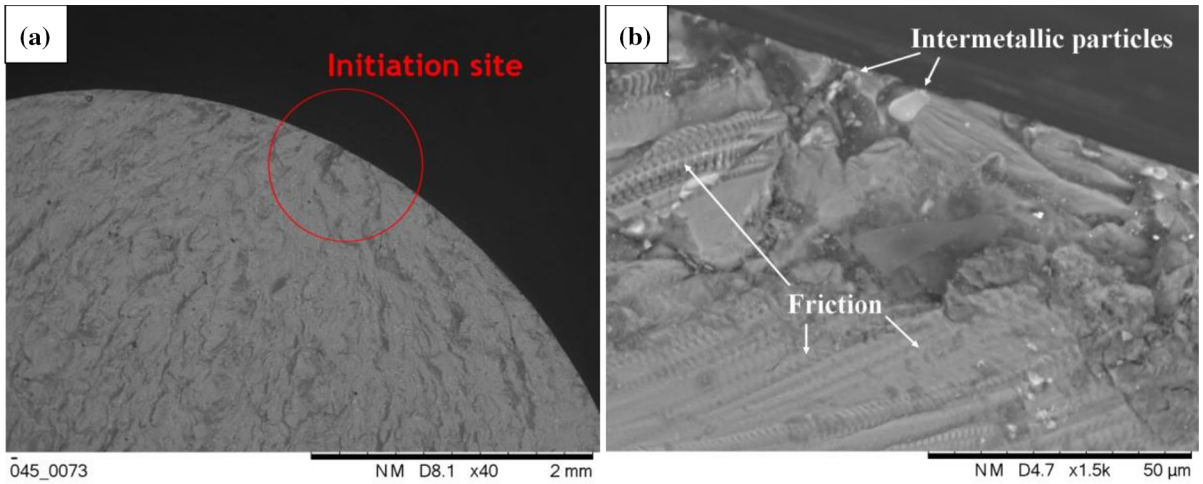

Fig. 18 Initiation site of machined specimen, τ_a = 85 MPa. **a** Full view of fracture and **b** initiation site localizations

(6) To conclude, the correlation between surface treatment, loading nature and their effect on fatigue life of 2618-T851 aluminum alloy is investigated. Results show that the surface crazing has no effect on fatigue life regardless of loading nature. Concerning the corrosion resistance, it is known that the coated substrate is less affected by corrosion than the uncoated substrate. The study of the influence of micro-cracks on the corrosion behavior was not the aim of the present paper.

Acknowledgements The author gratefully acknowledge Université Paul Sabatier for financial support of this research work and IRT-M2P in Metz (France) for making available the specimens and all surface treatments and in particular Joffrey Tardelli (IRT-M2P), Benjamin Mouls (IRT-M2P), Cédric Marchetto (IRT-M2P) and Aimé Ramakistin (INEOSURF).

References

Aghaie-Khafri M, Zargaran A (2010) Low-cycle fatigue behavior of AA2618-T61 forged disk. Mater Des 31:4104–4109. https://doi.org/10.1016/j.matdes.2010.04.043

Bathias C et al (1981) Influence of various parameters on the determination of the fatigue crack arrest threshold. Fatigue Eng Mater Struct 4:1–13

Boyer R, Welsch G, Collins EW (2007) Materials properties handbook: titanium alloys, 4th edn. ASM International, Materials Park

Canyook R, Seubsom P, Sang-ngean J, Trirujirapapong T, Taweesup K (2018) Influences of sealing solutions on anodized layer properties of 7075 aluminium alloy. Mater Today Proc 5(3):9483–9488

Cirik E, Genel K (2008) Effect of anodic oxidation on fatigue performance of 7075-T6 alloy. Surf Coat Technol 202:5190–5201. https://doi.org/10.1016/j.surfcoat.2008.06.049

Côté M-P, Benehkohal NP, Alpay N, Demopoulos GP, Brochu M (2014) Development of titanium-sputtered anodized aluminum substrates for dye-sensitized solar cells. Metall Mater Trans E 1(4):311–317. https://doi.org/10.1007/s40553-014-0032-7

Crawford BR (2013) Effect of anodising on the fatigue properties of aluminium alloys. Air Vehicles Division, Defence Science and Technology Organisation

Darmawan AS, Riyadi TWB, Hamid A, Febriantoko BW, Putra BS (2018) Corrosion resistance improvement of aluminum under anodizing process. AIP Conf Proc 1977:020006. https://doi.org/10.1063/1.5042862

Doyle WM (1969) The development of Hiduminium-RR58 aluminium alloy: the background to the choice of the main structural material for Concorde. Aircr Eng Aerosp Technol 41:11–14. https://doi.org/10.1108/eb034573

Fares C, Hemmouche L, Belouchrani MA, Amrouche A, Chicot D, Puchi-Cabrera ES (2015) Coupled effects of substrate microstructure and sulphuric acid anodizing on fatigue life of a 2017A aluminum alloy. Mater Des 86:723–734. https://doi.org/10.1016/j.matdes.2015.07.120

Goueffon Y, Arurault L, Mabru C, Tonon C, Guigue P (2009) Black anodic coatings for space applications: study of the process parameters, characteristics and mechanical properties. J Mater Process Technol 2(11):5145–5151. https://doi.org/10.1016/j.jmatprotec.2009.02.013

James MN, Hughes DJ, Chen Z, Lombard H, Hattingh DG, Asquith D, Yates JR, Webster PJ (2007) Residual stresses and fatigue performance. Eng Fail Anal 14:384–395. https://doi.org/10.1016/j.engfailanal.2006.02.011

Khalil O, Lang K-H (2011) Influence of microstructure on the quasistatic and low cycle fatigue behavior of an AA2618

aluminium alloy. Procedia Eng 10:1339–1347. https://doi.org/10.1016/j.proeng.2011.04.223
Kudari SK, Sharanaprabhu CM (2018) The effect of anodizing process parameters on the fatigue life of 2024-T-351 aluminium alloy. Fatigue Aircr Struct 2017(9):109–115
Liu W, Zuo Y, Tang Y, Zhao X (2008) The cracking behavior of anodic films on cast aluminum alloy after heating in the temperature range up to 300 °C. Surf Coat Technol 202:4183–4188. https://doi.org/10.1016/j.surfcoat.2008.03.008
Lonyuk B, Apachitei I, Duszczyk J (2007) The effect of oxide coatings on fatigue properties of 7475-T6 aluminium alloy. Surf Coat Technol 201(21):8688–8694. https://doi.org/10.1016/j.surfcoat.2006.02.002
Lu J, Wei G, Yu Y, Guo C, Jiang L (2018) Aluminum alloy AA2024 anodized from the mixed acid system with enhanced mechanical properties. Surf Interfaces 13:46–50. https://doi.org/10.1016/j.surfin.2018.08.003
Mason RB, Clark S, Klingenberg M, Berman E, Voevodin N (2011) Alternatives to dichromate sealer in anodizing operations. Met Finish 109(4–5):25–32
Mehdizade M, Soltanieh M, Eivani AR (2019) Investigation of anodizing time and pulse voltage modes on the corrosion behavior of nanostructured anodic layer in commercial pure aluminum. Surf Coat Technol 358:741–752
Nie B, Zhang Z, Zhao Z, Zhong Q (2013) Effect of anodizing treatment on the very high cycle fatigue behavior of 2A12-T4 aluminum alloy. Mater Des 50:1005–1010
Novy F, Janecek M, Kral R (2009) Microstructure changes in 2618 aluminium alloy during ageing and creep. J Alloys Compd 487(1–2):146–151. https://doi.org/10.1016/j.jallcom.2009.08.014
Özbek I (2007) A study on the re-solution heat treatment of AA2618 aluminium alloy. Mater Charact 58:312–317. https://doi.org/10.1016/j.matchar.2006.07.002
Schuster F, Lomello F, Billard A, Velisa G, Monsifrot E, Bischoff J, Ambard A, Brachet J-C, Lesaux M, Leflem M et al. (2015) On-going studies at CEA on chromium coated zirconium based nuclear fuel claddings for enhanced accident tolerant LWRS fuel. In: TopFuel 2015—Reactor Fuel Performance Meeting, Zurich, Switzerland cea-02492582
Shahzad M, Chaussumier M, Chieragatti R, Mabru C, Rezaï-Aria F (2010a) Influence of anodizing process on fatigue life of machined aluminium alloy. Procedia Eng 2:1015–1024. https://doi.org/10.1016/j.proeng.2010.03.110
Shahzad M, Chaussumier M, Chieragatti R, Mabru C, Rezaï-Aria F (2010b) Influence of surface treatments on fatigue life of Al 7010 alloy. J Mater Process Technol 210:1821–1826. https://doi.org/10.1016/j.jmatprotec.2010.06.019
Shahzad M, Chaussumier M, Chieragatti R, Mabru C, Rezaï-Aria F (2011a) Effect of sealed anodic film on fatigue performance of 2214-T6 aluminium alloy. Surf Coat Technol 206(11–12):2733–2739. https://doi.org/10.1016/j.surfcoat.2011.10.033
Shahzad M, Chaussumier M, Chieragatti R, Mabru C, Rezaï-Aria F (2011b) Surface characterization and influence of anodizing process on fatigue life of Al 7050 alloy. Mater Des 32(6):3328–3335. https://doi.org/10.1016/j.matdes.2011.02.027
Shiozawa K, Kobayashi H, Terada M, Matsui A (2000) Effect of anodized coatings on fatigue strength in aluminum alloy. Trans Jpn Soc Mech Eng A 66(652):2170–2175. https://doi.org/10.2495/SURF010371
Veys-Renaux D, Chahboun N, Rocca E (2016) Anodizing of multiphase aluminium alloys in sulfuric acid: in-situ electrochemical behaviour and oxide properties. Electrochim Acta 211:1056–1065. https://doi.org/10.1016/j.electacta.2016.06.131
Wang J, Yi D, Su X, Yin F (2008) Influence of deformation ageing treatment on microstructure and properties of aluminium alloy 2618. Mater Charact 65:965–968. https://doi.org/10.1016/j.matchar.2007.08.007
Wang R, Wang L, He C, Lu M, Sun L (2019) Studies on the sealing processes of corrosion resistant coatings formed on 2024 aluminium alloy with tartaric-sulfuric anodizing. Surf Coat Technol 360:369–375
Williams JC, Starke EA (2003) Progress in structural materials for aerospace systems. Acta Mater 51:5775–5799. https://doi.org/10.1016/j.actamat.2003.08.023
Zhang LM, Zhang SD, Ma AL, Hu HX, Zheng YG, Yang BJ, Wang JQ (2018) Influence of sealing treatment on the corrosion behavior of HVAF sprayed Al-based amorphous/nanocrystalline coating. Surf Coat Technol 353:263–273
Zhao X, Wei G, Yu Y, Guo Y, Zhang A (2015) An analysis of mechanical properties of anodized aluminum film at high stress, fatigue of aircraft structures. Surf Rev Lett 22(1):1550002